WAVEFORM DESIGN FOR MAXIMUM PASS-BAND ENERGY*

Steven R. Doctor, Alan G. Gibbs, R. Parks Gribble
Pacific Northwest Laboratories
Richland, Washington 99352

ABSTRACT

One way to maximize the sensitivity of an ultrasonic inspection is by establishing the pulser output voltage waveform to provide the maximum possible fraction of its energy in the pass-band of the piezoelectric transducer. An analytical study is reported that is backed up with experimental verification. Two pulser constraints are analyzed in this study. The first constraint is to study the common and easily generated waveform shapes for which each waveform has unit energy and compare to the optimum waveform shape with unit energy that is determined analytically. The second constraint is to repeat the first analysis with waveforms having unit amplitude rather than unit energy.

The analysis for the first constraint shows that the numerically intractable problem of summing a very large number of Fourier coefficients can be replaced by a mathematically equivalent evaluation of the pass-band energy which requires only the integration of smooth functions. This alternative formulation also leads to the result that the optimized waveform is the eigenfunction of a particular integral operator corresponding to the largest eigenvalue. The eigenvalue itself gives the maximum attainable pass-band energy. The optimized waveform is compared with sine waves, rectangular waves, trapezoidal waves, triangle waves and exponential spikes for 1/2, 1 and 3/2 cycle durations.

The analysis for the second constraint shows that the unit amplitude is in the form of an inequality which is outside the realm of the classical calculus of variations. An exact characterization of the optimized waveform was not found but numerical integration techniques were employed to determine the pass-band energies for the waveforms considered under the first constraint.

Finally, a breadboard pulser model is constructed and extensive comparisons of the various waveshapes, sensitivity studies, spectral distributions and experimental verification are made for each constraint.

INTRODUCTION

The Manufacturing Technology Program of the U.S. Air Force has undertaken a program to develop a reliable and advanced modular nondestructive testing system that will meet the current and future requirements of USAF Field/Depot NDE activities. As part of this program, a review and evaluation was made of all current technology for improving the performance of ultrasonic inspection equipment. Advances in electronic devices (i.e., high power FET devices) have made it possible to build compact, small, economical and high voltage pulsers capable of generating a variety of waveshapes.

For many years, a controversy has existed over which type of pulser output voltage waveform is the best signal to employ when driving a piezoelectric transducer. The solution to this controversy requires that many UT system parameters need to be evaluated, i.e., sensitivity, resolution, impedance matching, etc. The analysis reported here is for the theoretical optimum waveform design and other selected waveforms which can be generated in the laboratory. The results presented are backed up with laboratory experiments. The details of the analytical analysis are presented first for waveforms which have unit energy, next, the analysis for waveforms which have unit amplitude and finally, the laboratory results are presented.

As a part of the Manufacturing Technology Program of the U.S. Air Force, a survey was made of USAF Field/Depot NDE activities and it was found that the transducer employed in the largest number of inspections was a 5 MHz unit. The following analysis will use a transducer operating at 5 MHz, with a bandwidth of 40%. The 40% bandwidth is chosen because a transducer typical of the ones used by the USAF is available and it has a 41% bandwidth. Therefore, a transducer is available to provide experimental results for comparison with the theoretical results. Beside the data shows that the results would not change significantly for other bandwidths.

MAXIMUM PASS-BAND ENERGY FOR WAVEFORMS WITH UNIT ENERGY

The analysis presented here is in a general form that leads to a closed mathematical solution. Let $f(t)$ denote a function of period T and let $f(t)$ be zero for $\tau < t < T$ and periodic in T, as shown in Figure 1. The energy analysis proceeds by expanding $f(t)$ in a Fourier series and then, either integrating or summing the square of each frequency present to find the total energy (E_T). The fractional energy (E_F) in a particular frequency band can be found by summing or integrating only the frequencies contained in the band (E_B) and dividing by the total energy (E_T).

$$E_F = \frac{E_B}{E_T} = \frac{T \sum_{n \in N} (f_n)^2}{\int_0^t f^2(t)dt} \qquad (1)$$

*This work was sponsored by the Manufacturing Technology Division of the Air Force, Wright Aeronautical Laboratories, under Contract F33615-78-C-5032. For further information, contact Battelle Program Manager A.S. Birks (509) 375-2372 or the U.S. Air Force Program Manager R.R. Rowand (513) 255-5407.

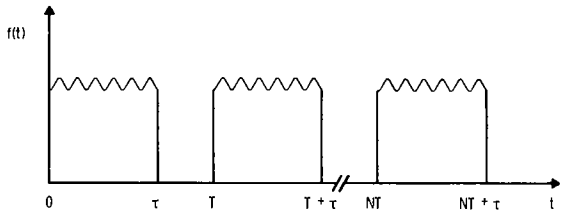

Fig. 1 Definition of the pulser output waveform.

This equation can be manipulated to yield:

$$E_F = \frac{\int_0^1 dx f(x) \int_0^1 dx' f(x') k(x-x')}{\int_0^1 f^2(x) dx} \qquad (2)$$

where $x = t/\tau$, $f(x) = |f(t)|_{t \to x\tau}$ and K is a kernel given by:

$$K(x) = \frac{2}{\pi} \ell\varepsilon_1 \frac{\sin \ell\varepsilon_2 x}{\sin \ell\varepsilon_1} \cos(\pi + \varepsilon_1) \qquad (3)$$

where

$$\varepsilon_1 = \pi/2\ FT \qquad (4)$$

$$\varepsilon_2 = \pi b/200 \qquad (5)$$

Note that K depends on three factors:

ℓ = length of signal in number of half-cycles of the driver frequency

FT = (driver frequency F) x (period T)

b = % bandwidth

This formalism has the advantage that the sum in equation (1) can now be performed in closed form. This formalism has replaced the problem of adding a very large number of $|f_n|^2$ with the easier problem of integrating smooth functions. An additional bonus is that an equation can be obtained for the optimum waveform.

The optimum waveform equation is derived by recognizing that the calculas of variations is applicable to equation (2). This leads to the conclusion that the maximum pass-band energy occurs when f(t) for $0 < t < \tau$ is the eigenfunction of the integral operator K corresponding to the largest eigenvalue. The resulting energy is the size of the eigenvalue. This formalism does not readily lend itself to solutions for various f(t)'s but numerical solutions can be easily obtained. Equation (2) was programmed on the VAX 11-780 computer using available library matrix routines. A Simpson's integration rule was used with good convergence observed on the largest few eigenvalues and eigenfunctions.

The results using numerical integrations are summarized in Table 1. The eigenfunctions for this problem cannot be written in the form of elementary functions. Hence, the optimum function is found numerically, which in this case is fortuitously quite similar to the elementary function sin πx. In reality, the optimum function and sin πx agree only to three figures and round off causes the apparent four figure agreement. For f(t) intervals with an integer multiple (ℓ), of center frequency half cycles, the optimum function is close to sin $\ell\pi x$ but the differences get larger as ℓ increases (see Table 3). In all cases, the differences are genuine, since the true eigenfunction is sin $\ell\pi x$ only in the limit as the bandwidth goes to zero. For all practical purposes, the first four waveshapes provide about the same energy in the 40% bandwidth. It is interesting to note that the exponential was the worst case.

Table 1
Comparison of Different Waveforms with Unit Energy for the Fractional Energy in a 40% Bandwidth

Waveform	Fractional Energy in 40% Bandwidth
Optimum f(x)	19.98%
Sin πx	19.98%
Trapazoid Wave	19.94%
Triangle Wave	19.68%
Square Wave	16.30%
Exponential (e^{-5x})	11.60%

Various trapezoids were evaluated and it was discovered that the symmetrical trapezoids are better than asymmetrical ones. For symmetrical trapezoids of the form shown in Figure 2, the numerical results are listed in Table 2. The limit of the "a" values lead to the square wave for a = 0 and the triangle wave for a = 1/2.

Table 2
Performance of Trapezoidal Waveforms

a Value	Fractional Energy in 40% Bandwidth
0 (rectangle)	16.3%
0.1	18.1%
0.2	19.4%
0.3	19.98%
0.33 (best)	19.94%
0.35	19.94%
0.4	19.87%
0.5 (triangle)	19.68%

Figure 3 shows the plots for four of the waveshapes of interest. This data shows that for other transducers with differing bandwidths, the efficiency for these waveshapes would all vary in about the same proportion, keeping the ordering in Tables 1 and 2 the same. It is also apparent from Fig. 3 why the exponential waveshape has been used extensively. First, the exponential wave is easy to generate and second, the power output remains more nearly constant over a very large frequency band.

Finally, some of the waveforms were examined for ℓ = 2, 3 etc. and these results are contained in Table 3. As ℓ increases, the effect is to

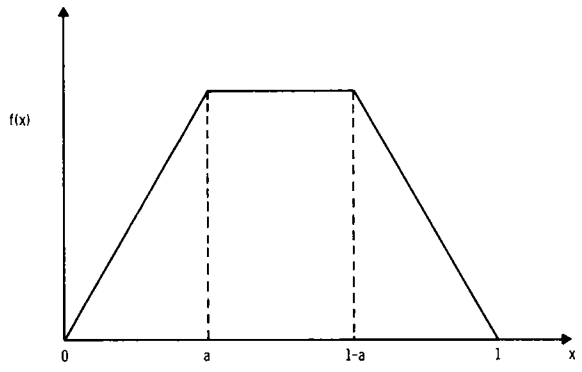

Fig. 2 Trapezoidal waveshapes.

narrow band the power spectrum and concentrate the power into the bandwidth of interest. The only exception was the exponential which provided the maximum power for $\ell = 2$.

MAXIMUM PASS-BAND ENERGY FOR WAVEFORMS WITH UNIT AMPLITUDE

This problem is related to one already solved but with the constraint in amplitude which satisfies:

$$|f(x)| \leq 1 \qquad (6)$$

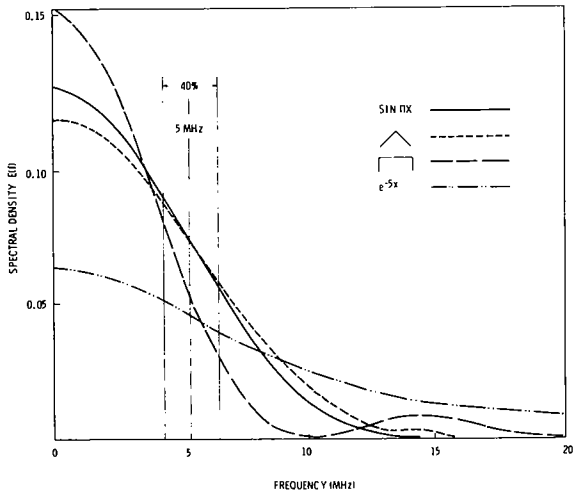

Fig. 3 Power spectral density for a sine wave, triangle wave, square wave and exponential.

Table 3
Fractional Power Supplied by Various Waveshapes for Integer Multiples of Half Cycles of the Center Frequency

	Fractional Energy in 40% Bandwidth for		
ℓ	Optimum f(x)	Sin $\ell\pi x$	$e^{-5t/\ell\tau 1/2}$
1	19.98%	19.98%	11.6%
2	38.67%	38.67%	12.42%
3	55.04%	54.98%	10.85%
4	68.47%	68.18%	8.97%
5	78.81%	77.97%	------

The objective is to determine the actual energy within the 40% bandwidth for various waveforms f(t). Ideally, we would like to find the waveform f(t) which maximizes E_F in equation (2), subject to the constraint of equation (6). However, this constraint is in the form of an inequality and makes this problem fall outside the realm of classical calcules of variations. Methods have been developed in the theory of optimal control for treating problems with inequality constraints but these approaches were not pursued. Instead, a numerical solution was obtained for the waveshapes described in the previous section. There was a change in the time constant for the exponential wave. The previous study used a time constant (5) such that the exponential was reduced essentially to zero in a time of one-half cycle of the center frequency. In the present study, an exponential time constant was selected so that the waveform decayed to one-half its initial amplitude in the same time as one-half cycle of the transducer's center frequency.

The total energy content of each signal can be found by calculating the denominator of equation (2). The integrals can all be performed in closed form and the results are shown in Table 4. Using numerical computer techniques as discussed in the previous section, the fractional energy can be determined. Table 5 contains those results. It is interesting to note that although some of the waveforms are very efficient at getting their available energy into the pass-band (trapezoid, sine and triangle waves), they do not produce maximum pass-band energy. This results from the fact that the total available energy from each waveform is different. Consequently, the waveform which produces the highest pass-band energy appears to be the superior pulse driver waveshape.

Table 4
Total Energy for the Waveforms Shown

Waveform	$E_T = \int_0^1 f^2(x)dx$
Square	a(1.0 for a = 1)
Trapezoid	$1-\frac{4}{3}a$ (5/9 for a = 1/3)
Triangle	1/3
Sin $\ell\pi x$	1/2 (independent of ℓ)
Exponential	$(1-1/4^{\ell})/Ln4^{\ell}$

Figures 4 and 5 contain the power spectral density plots for the waveforms considered. It is apparent from these figures why the square wave is by far the best waveform to be used for maximizing pass-band energy.

TABLE 5

Total Energy E_T, Fractional Energy E_F and Pass-Band Energy E_B for the Waveform Shown

Waveform	E_T	E_F	E_B
Square	1.000	0.1631	0.1631
Trapezoidal (a = 1/3)	0.5555	0.1994	0.1107
Sin πx	0.5000	0.1998	0.09989
Triangle	0.3333	0.1968	0.06568
Exponential	0.7213	0.05582	0.04026

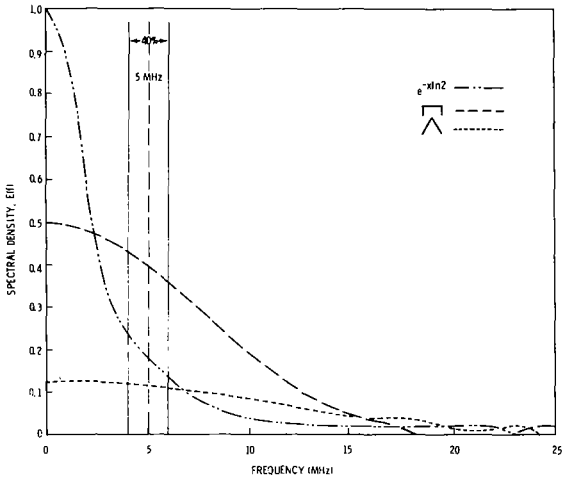

Fig. 4 Power density spectral plot for the square, triangle and exponential waves.

EXPERIMENTAL RESULTS

To verify the results predicted by the two studies reported above, laboratory tests were performed. It is very convenient to generate in the laboratory, waveforms which have the same peak amplitude. However, it is extremely difficult to make the driver output energy equal for the different waveshapes because the piezoelectric transducer is a nonlinear complex load and this creates significant distortions in the driver pulse shape. Consequently, the results reported here will only be for equal driver pulse amplitudes. Furthermore, the two limiting cases in the unit amplitude study are the square wave and the exponential. These two curve shapes were studied in detail.

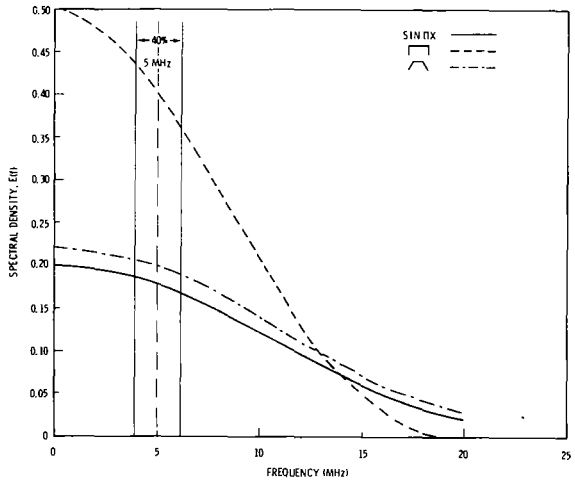

Fig. 5 Power density spectral plot for the square, trapezoidal and sin wave.

The transducer selected is 1/4" x 1/4", designed to operate at 5 MHz, Model No. HMT 7-221. This transducer operated at 4.65 MHz and had a 41% bandwidth as measured with a tone burst method (Ref. 1). A six foot RG-174/u cable was used and an insertion loss of -30 dB was measured and an impedance of Z = 70 ohms ∠ 20° was measured.

The exponential pulse is generated with a Metrotek MP-215 (typical of SCR shock type pulsers) pulser whose output impedance was approximately 10 ohms. The pulse amplitude control is adjusted to 85 V and the damping control is adjusted to provide a pulse whose duration (measured at 50% levels) is set equal to one-half cycle of the center frequency. The exponential has a 20 ns risetime, 120 ns width and an overall duration of 650 ns.

A circuit was developed at Battelle to generate square waves and this circuit provides a control to adjust the width of the square wave. The square wave has an amplitude of 85 V, a risetime of 16 ns and a fall time of 12 ns. The pulser has an output impedance of approximately 13 ohms. The pulser has a width control which was adjusted to give a maximum response from a quartz block submerged in water (a duration of 114 ns).

If we review the theoretical results of the previous section, then there should be a 6 dB difference for the two pulser waveshapes. Comparison of the two pulsers by examining the responses from a quartz block indicated that the return echo amplitude and shape is identical in both cases (see Fig. 6). There are several reasons for the discrepancy (lack of 6 dB difference) between the theoretical and laboratory results. The most important reason is the difference between the exponential waveshape which is generated in the lab and the mathematical exponential wave used for

the calculations as shown in Fig. 6. The mathematical exponential wave has an infinite risetime and decays exponentially from unity. The laboratory exponential wave is rounded and does not start its decline for approximately 30 ns. If, at the 50 ns point, the exponential is projected back to find the peak value, then the exponential would be equivalent to starting its decline from 120 V at time zero. This provides an additional 6 dB of power because of the square relationship of equation (1). The 6 dB of additional power offsets the theoretically predicted 6 dB loss in sensitivity. In general, the shape of a spike pulse will differ considerably for reactive loads from a pure exponential decay. Thus, a spike pulse achieves improved performance by providing more power in the pass-band.

It is important to note that even though there is no sensitivity improvement (i.e., no dB improvement) with the square wave pulser under ideal conditions for the spike pulser, there are several very attractive reasons why it is the best pulser to use. First the square wave pulser does not saturate the front end of the receiver amplifier at the end of the drive pulse because the pulse is driven to and held at 0 V. Consequently, for contact inspection, the near surface resolution is substantially improved. Secondly, the square wave pulser can be easily tuned (via width control) to the operating frequency of the transducer without affecting the voltage amplitude, the waveshape or the output impedance of the pulser. This feature enhances interchangeability of transducers for producing identical UT responses from calibration reflectros and defects.

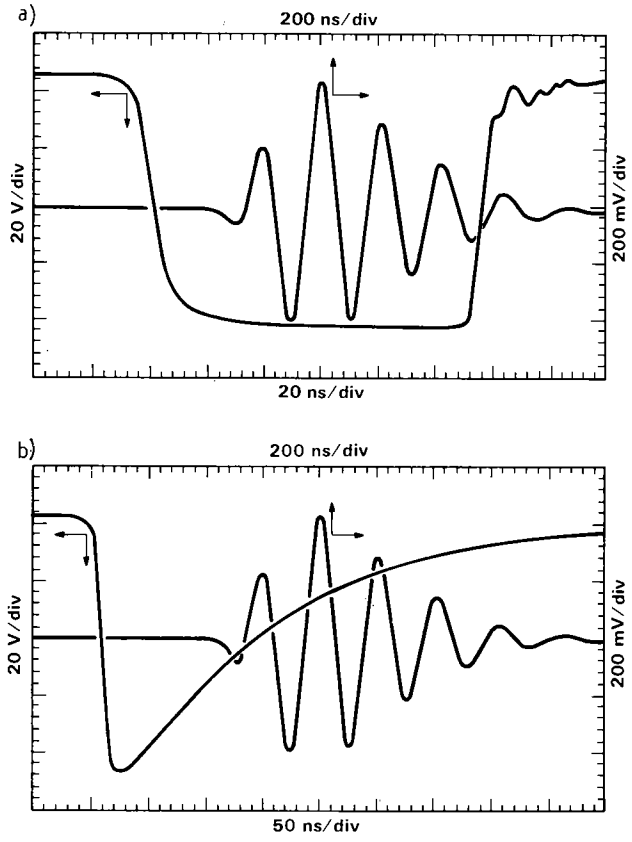

Fig. 6 Pulser output shape and return echo for (a) square wave, and (b) spike (exponential.

CONCLUSIONS

The analytical study using the constraint of unit energy for each waveform, leads to the conclusion that the optimum f(x), sin πx, trapezoid (a = 1/3) and the triangle wave each had essentially the same fraction of energy in the 40% bandwidth. As the number of half-cycles of the transducer center frequency is increased, the fractional energy in the 40% bandwidth increases.

The analytical study using the constraint of unit amplitude for each waveform leads to several conclusions. The first conclusion is that the square wave has the largest total energy E_T, the sin πx wave has the highest efficiency E_F for getting energy in the pass-band but the square wave has the highest pass-band energy E_B. The second conclusion is that the spike pulse exponential wave has 6 dB less energy in the pass-band than the square wave.

Experimental results for the square wave and the exponential wave turned out to be identical. The difference between the mathematical exponential and the experimental exponential pulse results is 6 dB more power in the pass-band, thus, equaling the square wave configuration. The spike pulse waveshape is typical of SCR pulsers and provides the power in the pass-band that allows them to work satisfactorily into a reactive load.

The square wave pulser, on the other hand, possesses several advantages even though in the particular instance studied, no sensitivity improvement is realized. The square wave pulser reduces the need to tailor the waveform and eliminates distortions caused by the exponential decay, thus providing improved near surface resolution and improved UT test reporducibility. Further, the square wave pulser can be optimized to the operating frequency of the transducer by tuning without changing the electrical impedance or other electrical properties of the pulser network. However, the operating and electrical characteristics for the spike pulser change with adjustments to the pulse duration.

ACKNOWLEDGEMENTS

The authors wish to thank Charles A. Ratcliffe for designing the square wave pulser circuit and Paul L. Tomeraasen for building the circuit for testing.

REFERENCES

1. Erickson, K.R., "Tone-Burst Testing of Pulse Echo Transducers," IEEE Transactions on Sonics and Ultrasonics,Vol. SU-26, No. 1, pp. 7-14, January, 1979.